Journal of Materials Chemistry

Cite this: J. Mater. Chem., 2011, 21, 13561

www.rsc.org/materials

PAPER

A novel fluorogenic hybrid material for selective sensing of thiophenols†

Wenwen Zhao,[a] Weimin Liu,[a] Jiechao Ge,[a] Jiasheng Wu,[a] Wenjun Zhang,*[b] Xiangmin Meng[a] and Pengfei Wang*[a]

Received 22nd April 2011, Accepted 17th June 2011
DOI: 10.1039/c1jm11768h

A fluorogenic organic-inorganic hybrid sensory material (denoted as material **III**) was successfully prepared by immobilizing disulfide-based receptors within the channels of mesoporous silica MCM-41. The material showed high sensitivity and excellent selectivity towards thiophenols due to appropriate combination of the stronger nucleophilicity of thiophenols and the secondary interactions (hydrophobicity and π–π stacking interactions) provided by the inorganic support. Fluorescence measurements revealed that the emission intensity of material **III** increased significantly upon addition of thiophenols, while it was not observed for aliphatic thiols and other nucleophiles. The detection limit of this material to *p*-toluenethiol was estimated to be 7.4×10^{-6} M, and a good linear relationship between the fluorescence intensity and *p*-toluenethiol concentration (in the range of 0–110 μM) was achieved. The pronounced emission enhancement could be attributed to the following conversion process: a coumarin derivative is released from material **III** by cleaving the disulfide bonds in the presence of thiophenols, and then oxidized spontaneously to a fluorescent dye (coumarin 6) under ambient conditions. This novel sensing method *via* disulfide-based groups as the active site combining with the synergistic effect provided by the inorganic support is expected to open a new avenue for thiophenols sensing.

Introduction

Development of sensing techniques for chemical species by employing sophisticated molecular recognition systems has been one of the most active areas in supramolecular chemistry. Among them, chromogenic and fluorogenic sensors for detecting various cations, anions, and neutral species have attracted great attention due to their high sensitivity, selectivity, as well as their on-line and real-time analysis capabilities.[1–5] In recent years, organic-inorganic hybrids prepared generally by immobilizing organic receptors on inorganic supports of nanometre scales have been a class of extremely promising materials for molecular recognition.[6–12] Structurally well-defined mesoporous silica materials such as MCM-41 and SBA-15 are among the most charming solid supports owing to their large surface area, high thermal stability and specific structure of channels. Thus far, there have been many reports on cation sensing *via* grafting fluorescent molecules on the surface or into the nanochannels of mesoporous silica.[13–17] However, only limited examples of such heterogeneous sensors for detecting anions or neutral species have been shown.[18–20]

Recently, by utilizing the predefined chemical binding center together with the selected properties of the mesoporous silica, an enhanced selectivity to detect guest species with similar molecular structures has been reported.[21] This approach is especially attractive due to the employment of molecular-solid synergistic effects that are difficult to achieve by only molecular-based systems or in nanoscopic solids. In the reported sensory systems, mesoporous supports could provide some additional interactions, such as size-sieving effect, hydrophobic/hydrophilic property, π–π interaction, or their combined effect.[18,22–24] As a prominent enhancement of selectivity based on the synergistic effect, Lin *et al.* designed and synthesized the OPTA-derived mesoporous silica materials, and demonstrated that the substrate accessibility could be modulated simultaneously by creating a different pore micro-environment. As a result, its selectivity to the similar bio-molecules such as dopamine and glucosamine was enhanced.[22] Martínez-Máñez *et al.* also prepared several sensory materials for the selective detection of long-chain carboxylates, specific amines,[24,25] and ATP (adenoisine 5′-triphosphate)[18,26] among their analogues by coupling the selected organic

[a]*Key Laboratory of Photochemical Conversion and Optoelectronic Materials, Technical Institute of Physics and Chemistry, Chinese Academy of Sciences, Beijing, 100190, P. R. China. E-mail: wangpf@mail.ipc.ac.cn; Tel: +010-82543435*
[b]*Center of Super-Diamond and Advanced Films (COSDAF) and Department of Physics and Materials Sciences, City University of Hong Kong, Hong Kong SAR, P. R. China. E-mail: apwjzh@cityu.edu.hk*

† Electronic supplementary information (ESI) available: Preparation of material **I**; Synthesis and characterization of compounds **2** and **3**; Analysis of the TGA of materials; Calculation of the detection limit and measurements of the response time for material **III** towards *p*-toluenethiol; ESI-MS and ^{1}H NMR spectrum analysis to prove the formation of coumarin 6. See DOI: 10.1039/c1jm11768h

molecules with the additional interactions provided by mesoporous solids.

Herein, we report a new organic–inorganic hybrid sensory system (material **III** as shown in Scheme 1a) which enables a highly selective detection of thiophenols over aliphatic thiols and other nucleophiles. Thiophenols have been widely used as a chemical intermediate for pesticides, pharmaceuticals, and amber dyes.[27–30] Long-term exposure to thiophenols can cause severe damage to the central nervous and other nervous systems including shortness of breath, muscular weakness, paralysis of the hind limbs, coma, and even death.[31–33] The median lethal dose (LC50) of thiophenols ranges from 0.01 to 0.4 mM for fish,[34] and thiophenol has been added to the priority lists of pollutants by the United States Environmental Protection Agency (USEPA) (EPA waste code: P014).[35,36] Although a number of fluorescent probes for sensing thiols have been reported,[37–44] they exhibit poor selectivity towards thiophenols and aliphatic thiols. Thus far, there are only few examples of fluorescent probes showing high selectivity toward thiophenols,[45–47] and they are all built with relatively simple molecular systems. Therefore, it is significant to develop new sensory systems to discriminate thiophenols over aliphatic thiols in environmental analysis. In our current approach, the disulfide-based group is selected as the receptor which can be selectively cleaved by thiol-containing compounds.[39,48–50] We expect that anchoring of this unique receptor on the pore surface of mesoporous silica MCM-41 could provide some additional interactions in the solid surface, including hydrophobic and π–π stacking interactions, which could further enhance its sensitivity and selectivity to thiophenols. The experimental results demonstrate that addition of thiophenols results in a significant emission enhancement of material **III**, while there is no gain for aliphatic thiols and other nucleophiles under the same conditions. To illustrate clearly the necessity of the solid supporting matrix, model compound **4** (Scheme 1b) was also synthesized for a comparable illustration of its fluorescent response towards *p*-toluenethiol.

Experimental

Reagents and materials

2,2′-Dipyridyl disulfide, 2-aminothiophenol, tetraethoxysilane (TEOS), cetyltrimethylammonium bromide (CTAB), 3-mercaptopropyltrimethoxysilane (MPTES), and all analytical chemicals, including cysteine, gluotathione, glycine, phenol, aniline, *n*-propylmercapatan, *p*-nitrothiophenol, *p*-chlorobenzenethiol, *p*-methoxythiophenol and *p*-toluenethiol, were purchased from Alfa Aesar. Other reagents were purchased from Beijing Chemical Regent Co. All reagents and chemicals were AR grade and used directly without further purifications unless otherwise noted. Ethanol used for measurement is of chromatographic grade, and water was purified by Millipore filtration system. The metal cations for interference determination were all of perchlorate salts.

Instruments and spectroscopic measurements

^{1}H NMR and ^{13}C NMR spectra were obtained on a Bruker Advance 400 NMR spectrometer using tetramethylsilane (TMS) as an internal reference. Electron impact (EI) mass spectra were recorded on a Waters GCT Premier mass spectrometer and electrospray ionization (ESI) mass spectra on a Shimadzu LC-MS2010 instrument. FT-IR spectra (4000–400 cm^{-1}) were collected on a Varian Excalibur 3100 FTIR spectrometer. Thermogravimetric analysis of the samples was carried out on a TA TGA 2050 with a nitrogen flow of 100 mL min^{-1} at a rate of 10 °C min^{-1} from room temperature to 900 °C. Elemental analysis (C, H, N) was performed on an Elementar Vario EL III analyzer. Small-angel XRD measurements were performed on a X'Pert PRO X-ray diffractometer using Cu-Kα radiation (λ = 1.5418 Å) at 40 kV and 10 mA. TEM spectra were recorded on a JEOL JEM-2100 at an acceleration voltage of 150 kV. The nitrogen adsorption-desorption isotherms were measured at 77 K on a QuadraSorb SI automated surface area and pore size analyzer. And the samples were degased under vacuum at 423 K

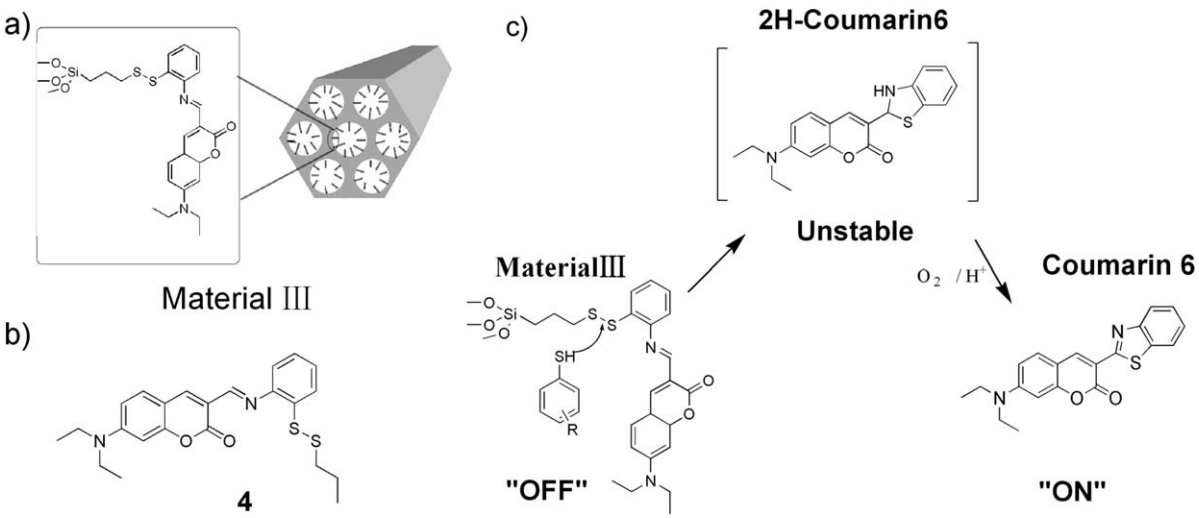

Scheme 1 Structures of a) material **III** and b) model compound **4**, and c) the proposed sensing mechanism for material **III** towards thiophenols.

for 4 h before measurements. Surface areas were calculated based on the Brunauer-Emmett-Teller method, and the pore size distribution were calculated using the Barrett–Joyner–Halenda (BJH) model on the desorption branch. The pore volumes were taken at the $P/P_0 \approx 0.99$. UV-visible spectra and fluorescence spectra were obtained with Hitachi U-3010 and F-4500 spectrophotometers, respectively. All spectrophotometric spectra of hybrid sensory material **III**, including fluorescence titration and the selectivity, were performed with a suspension of sample dispersed in a citric acid (0.1 M)-phosphate (0.2 M) buffer (pH 3, ethanol/water = 1/4, v/v), and all data were acquired at 30 min after the addition of target analytes. (Fig. S1†)

Synthesis of material I

Material **I** was prepared according to reported procedures.[51] The details for the synthetic process are described in the ESI†.

Synthesis of the amine-functionalized material II

Material **II** was synthesized by co-condensation under basic conditions using CTAB as surfactant templates, TEOS and organosilane **2** as co-condensed precursors. The molar ratio of reagents was CTAB : NaOH : TEOS : organosilane **2** : H_2O = 1.0 : 4.9 : 10.1 : 0.97 : 9356.8. As a typical procedure, CTAB (0.1 g) was dissolved in deionized water (48 g), and then NaOH (0.7 mL, 2 M) was added with vigorous stirring at room temperature. After the solution was heated at 80 °C for 30 min, a mixture of TEOS (0.6 g) and organosilane **2** (0.1 g) was poured into the solution while stirring vigorously. A yellowish precipitate was observed after 2 min and the mixture was continuously stirred for 2 h. After cooling to room temperature, the white solid products were isolated by filtration, washed thoroughly with water, and dried under vacuum for 4 h at 40 °C. The surfactant was removed by acid/solvent extraction in a methanol (15 mL) containing aqueous HCl (0.15 mL, 37.5%) solution. The mixture was stirred at room temperature for 24 h, washed with methanol several times after being filtered, and then dried in a vacuum. Elemental analysis, found: N, 1.545%, C, 19.35%, H 2.910%.

Synthesis of the fluorophore-grafted material III

Material **III** was prepared by anchoring the fluorophore to material **II**. 3-Formyl-coumarin (24.5 mg, 0.1 mmol) and material **II** (0.1 g) were dissolved in ethanol (10 mL). The color of the solution turned to bright red from light yellow immediately. The mixture was stirred for 8 h at room temperature. Then the resulting red solid was collected by centrifugation and washed with ethanol for about ten times to remove unreacted 3-formyl-coumarin. Elemental analysis, found: N, 1.301%, C, 15.24%, H, 2.685%.

Synthesis of 2-(pyridin-2-yldisulfanyl)benzenamine (1)

Compound **1** was synthesized from a thiol-disulfide exchange reaction. In a typical preparation process, 2,2′-dipyridyl disulfide (2.2 g, 10 mmol) was dissolved in dry CH_2Cl_2 (30 mL) and a solution of 2-aminothiophenol (1.5 mL, 12 mmol) in dry CH_2Cl_2 (15 mL) was injected dropwise at room temperature within about 40 min under nitrogen atmosphere. The initially colorless solution turned to yellow immediately after the addition of 2-aminothiophenol due to the formation of pyridine-2-thione. The mixture was stirred at room temperature for 3 h. After removal of the solvent by rotary evaporation, the residue was dropped into 50 mL of petroleum ether under vigorous ultrasonic vibration, and then was filtered. The filtrate was evaporated to produce the crude product, which was purified by column chromatography on silica gel (Eluent: dichloromethane/ethyl acetate = 100/2, v/v) to give **1** (1.1 g, 47%) as a yellowish liquid. ^{1}H NMR ($CDCl_3$, 400 MHz, δ): 8.51 (d, 1H, pyridyl-H), 7.49–7.58 (m, 3H, pyridyl-H), 7.08–7.16 (m, 2H, Ar-H), 6.61–6.70 (m, 2H, Ar-H), 4.92 (br, 2H, NH_2). ^{13}C NMR ($CDCl_3$, 100 MHz, δ): 159.0, 149.6, 149.2, 136.8, 136.2, 131.6, 121.1, 118.2, 118.0, 115.7. MS (ESI, *m*/*z*): $[M + H]^+$, calcd for $C_{11}H_{10}N_2S_2$, 234.0, found, 235.0.

Synthesis of 2 and 3

The processes for synthesis of organosilane **2** and compound **3** were similar to the process for compound **1** described above. The details for the synthetic process and characterization are described in the ESI†.

Synthesis of (E)-7-(diethylamino)-3-((2-(propyldisulfanyl) phenylimino)methyl)-2*H*-chromen-2-one (4)

Compound **4** was synthesized from a condensation reaction of compound **3** and 3-formyl-coumarin. A mixture of 3-formyl-coumarin (98 mg, 0.4 mmol) and **3** (0.12 g, 0.6 mmol) in ethanol (10 mL) with glacial acetic acid (1 mL) was refluxed for 8 h, and then cooled to room temperature. The dark red precipitates were collected, washed with cold ethanol, and purified by recrystallization from ethanol to yield 68 mg (40%) of **4** as a wine red solid. m.p: 128–130 °C. ^{1}H NMR (DMSO-d_6, 400 MHz, δ): 8.56 (s, 1H, coumarin-H), 8.50 (s, 1H, CH═N), 7.76 (dd, 1H, J = 7.5 Hz, J = 1.0 Hz, benzo-H), 7.73 (d, 1H, J = 8.9 Hz, coumarin-H), 7.28 (m, 2H, benzo-H), 7.16 (dd, 1H, J = 7.4 Hz, J = 1.0 Hz, benzo-H), 6.82 (dd, 1H, J = 2.2 Hz, J = 8.9 Hz, coumarin-H), 6.62 (d, 1H, J = 2.1 Hz, coumarin-H), 3.50 (q, 4H, J = 7.0 Hz, $2NCH_2$), 2.73 (t, 2H, J = 7.2 Hz, SCH_2), 1.63(m, 2H, SCH_2CH_2), 1.16 (t, 6H, J = 7.0 Hz, $2NCH_2CH_3$), 0.93 (t, 3H, J = 7.2 Hz, $SC_2H_4CH_3$), ^{13}C NMR ($CDCl_3$, 100 MHz, δ): 162.4, 157.9, 154.4, 152.2, 148.8, 142.0, 133.1, 131.3, 126.8, 126.8, 125.4, 117.8, 115.2, 109.8, 109.1, 97.3, 45.2, 40.8, 22.6, 13.3, 12.6. MS (HR-EI, *m*/*z*): $[M]^+$, calcd for $C_{23}H_{26}N_2O_2S_2$, 427.1436, found, 427.1440.

Results and discussion

Synthesis and characterization of materials I–III

The synthetic pathway is shown in Scheme 2. To explore the characters of the organic-inorganic hybrid sensory material **III**, we prepared a typical MCM-41-type material **I** as a contrast according to the literature, as shown in Scheme 2a.[51] Amine-functionalized material **II** was synthesized from the co-condensation of tetraethoxysilane (TEOS) and organosilane **2**. The co-condensation method allows the organic functional groups to be anchored homogeneously into the mesopore channels,[52,53] which is beneficial to the creation of a unique pore micro-environment. Finally, by the reaction of the amine groups of material **II** to the

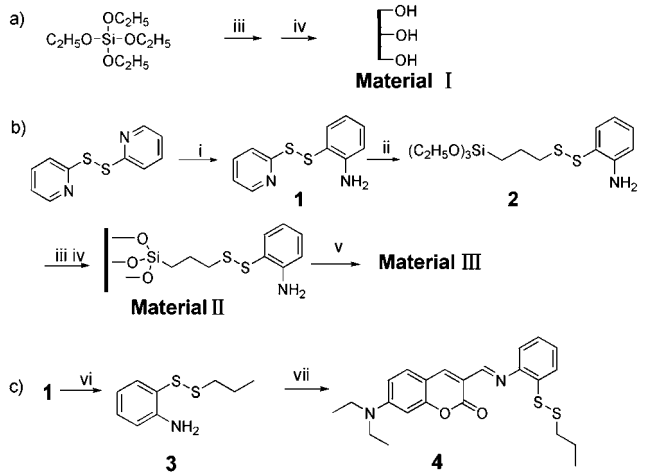

Scheme 2 Synthetic pathways for materials **I**, **II**, **III**, and model compound **4**. (i) 2-aminothiophenol, CH_2Cl_2, rt, 4 h; (ii) 3-mercaptopropyltriethoxysilane, CH_2Cl_2, rt, 4 h; (iii) TEOS, H_2O/NaOH (2 M, aq), 80 °C, 2 h; (iv) HCl/MeOH, rt, 24 h; (v) 3-formyl-coumarin, EtOH/HOAc, 60 °C, 8 h; (vi) $CH_3(CH_2)_2SH$, CH_2Cl_2, rt, 4 h; (vii) 3-formyl-coumarin, EtOH, rt, 8 h.

aldehyde groups of 3-formyl-coumarin, as illustrated in Scheme 2b, material **III** was obtained as a bright red solid. Moreover, model compound **4** (Scheme 1b) was designed and synthesized *via* a two-step thiol-disulfide exchange reaction (Scheme 2c).[54,55] Compound **2** was synthesized following the similar procedure of that of compound **4** and the fluorophore 3-formyl-coumarin was prepared according to the literature.[56] Further details for synthesizing materials **I–III** and the compounds **1–4** are described in the experimental section or ESI†.

Fourier transform infrared (FTIR) spectra of materials **I–III** are shown in Fig. 1. A peak at 1632 cm^{-1} is observed in all the spectra, which is ascribed to the –OH bending vibration of adsorbed H_2O.[57] The typical Si–O–Si band in materials **I–III** appears as three peaks: one broad and strong peak centered at 1084 cm^{-1}, and two narrow and relatively weak peaks near 801 and 468 cm^{-1}, which are associated with the condensed silica network.[58] Compared with the FTIR spectrum of material **I**, material **II** exhibits several new peaks at about 2929, 2856, 1484, 1447, and 1411 cm^{-1}, which are assignable to aliphatic C–H stretching and bending vibrations, suggesting the successful functionalization of material **II** with compound **2** by the co-condensation method. For material **III**, in addition to C–H vibrations bands at 2800–3000 and 1300–1500 cm^{-1}, the C=N and C=O stretching vibrations at 1607 and 1708 cm^{-1}, respectively, and the peaks at 1574 and 1532 cm^{-1} originating probably from the C=C stretching of the phenyl ring, are also observed. The above results provide a clear evidence that 3-formyl-coumarin is indeed attached to the pore surface of material **II**. The content of incorporated coumarin-residues was determined by thermogravimetric analysis (TGA) and elemental analysis (EA). According to the EA results, material **III** was estimated to contain approximately 3.91 wt.% of coumarin-residues, which agreed well with the content from thermogravimetric analysis (Fig. S2†). As a result, 100 ppm material **III** in aqueous solution corresponds to about 1.8×10^{-5} M of receptor.

Fig. 2 presents small-angle X-ray diffraction (SAXRD) patterns of materials **I–III**. Three well-resolved diffraction peaks of 100, 110, 200 and a weak peak of 210 were observed in material **I**, suggesting a 2-dimensional (2D) hexagonal symmetry (*p6mm*) and a long-range ordering of the mesoporous structure.[59] For the functionalized material **II**, the similar diffraction peaks at 100, 110 and 200 remain observable, indicating the same 2D hexagonal mesoporous structure of material **II** synthesized by the co-condensation method. Compared with material **II**, the diffraction peak 100 of material **III** keeps its original shape, indicating that the 2D-hexagonal ordering has been retained after grafting with the fluorophore. However, obvious decreases in intensity of all the peaks were observed in material **III**. Such a decrease might be ascribed to the lowering of local mesoporous ordering, such as the variations in the wall thickness, or it might be due to the reduction of scattering contrast between the channel walls and pore-filling material.[52] Thus, it can be understood as an indirect evidence for the successful coupling of fluorophores to the aniline groups inside the channels.

Fig. 3a displays the nitrogen adsorption-desorption isotherms for samples **II** and **III**. The isotherm of material **II** shows two sharp capillary condensation steps (at intermediate and high P/P_0 values) related to a bimodal pore system. The first step originates from the condensation of the nitrogen into the mesopores and the second one from the condensation inside the large

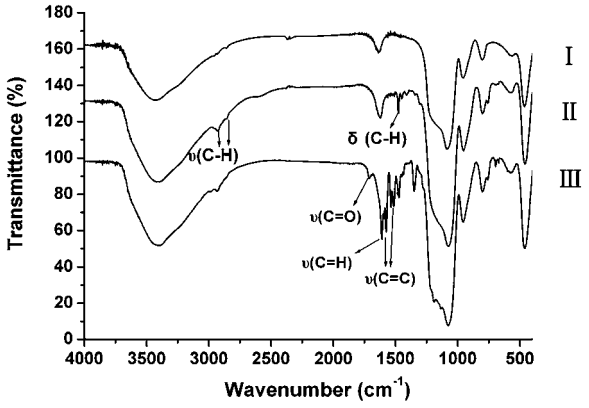

Fig. 1 FTIR spectra of materials **I**, **II**, and **III**.

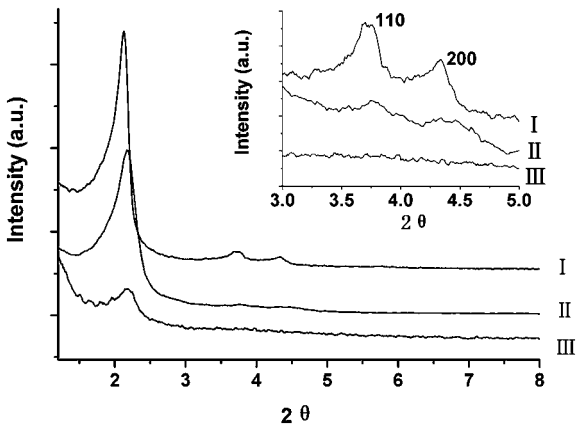

Fig. 2 SAXRD patterns of materials **I**, **II**, and **III**.

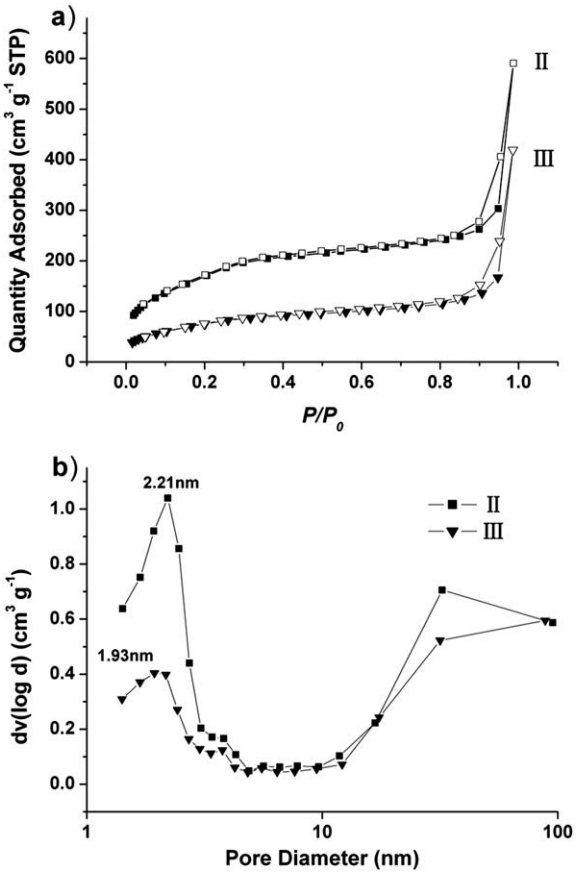

Fig. 3 a) N_2 adsorption (solid)-desorption (hollow) isotherms, and b) pore size distributions of materials **II** and **III**.

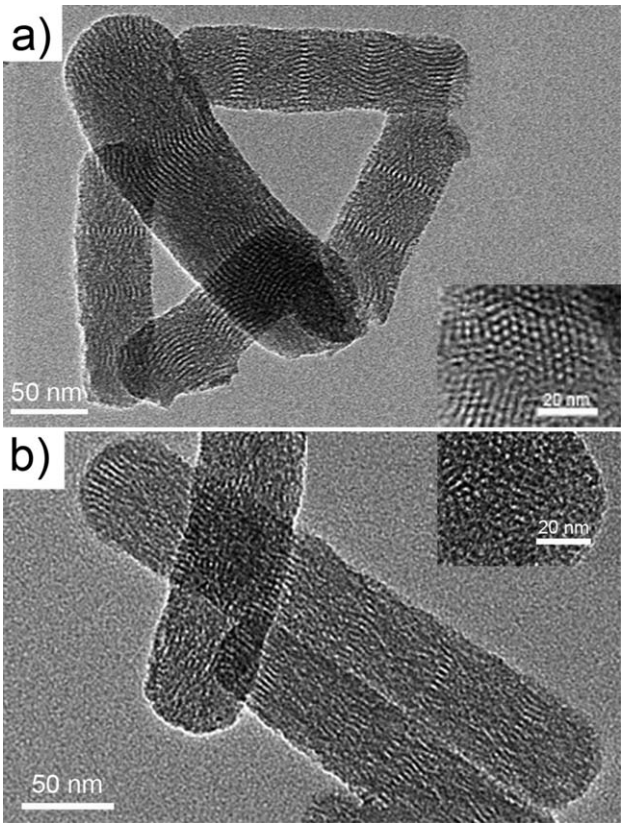

Fig. 4 TEM images of a) material **II**, and b) material **III**. Insets are the corresponding images obtained along the rod axis directions.

interparticle pores.[23,59] Consequently, pore size distribution (PSD) of this sample reveals bimodal pore diameters of *ca.* 2.21 and 32.22 nm, respectively (Fig. 3b). Comparing material **III** with material **II**, the isotherm and PSD pattern are almost retained, suggesting that the structural ordering of the channels was unchanged after grafting. But the decrease in the peak intensity and corresponding pore diameter (1.93 and 31.65 nm for material **III**) clearly suggests that the chromophores are grafted inside the mesopores, which agrees well with the observation in SAXRD. The corresponding structural parameters are summarized in Table S1†. Comparing material **III** with **II**, the Brunauer–Emmett–Teller (BET) surface area decreases from 621.0 to 270.3 $m^2\ g^{-1}$ and pore volume shrinks from 0.92 to 0.65 $cm^3\ g^{-1}$. The remarkable decreases in surface area and pore volume also support the conclusion that the fluorophores are indeed attached to mesopore surfaces and the void space is occupied.

The microstructures of materials **II** and **III** were studied by transmission electron microscopy (TEM), as shown in Fig. 4. It is interesting to note that material **II** is in the morphology of helicalmesostructured rods. The image obtained with the incident beam perpendicular to the pore axis illustrates the appearance of lattice fringes, indicating the presence of chiral channels within the helical rods.[60,61] Observation along the pore axis direction reveals well-aligned mesopores in a highly-ordered 2D-hexagonal symmetry (inset in Fig. 4a), which is well consistent with the SAXRD result. After grafting of fluorophores (material **III**), the image of lattice fringes and pore-ordering remain observable (Fig. 4b), which confirms that hexagonal ordering has been preserved after the introduction of fluorophores.

Fluorescence response of material III towards thiophenols

Fluorescence titration experiments were carried out to illustrate the emission response of material **III** to the various concentrations of *p*-toluenethiol, as shown in Fig. 5a. The emission peak intensity at *ca.* 500 nm increases monotonically with a "red shift" with the increase of *p*-toluenethiol concentration. Fig. 5b shows the dependence of fluorescence intensity at 512 nm on the *p*-toluenethiol concentration. A linear relationship ($R = 0.994$) for the concentrations ranging from 0 μM to 110 μM was observed (inset in Fig. 5b), implying that material **III** is very promising in the quantitative analysis of thiophenols. Furthermore, the detection limit of material **III** for sensing *p*-toluenethiol was determined to be as low as 7.4×10^{-6} M (Fig. S3†), which can meet the practical requirement for detecting thiophenols on the submillimolar level in environmental analyses.[34]

The proposed sensing mechanism of material **III** to *p*-toluenethiol is depicted in Scheme 1c. Upon the addition of thiophenols, the disulfide bond is facilely cleaved by thiophenols and a coumarin-based compound (2*H*-coumarin 6) is released to the solution, which is spontaneously oxidized to a laser dye (coumarin 6) under ambient conditions. To confirm the formation of coumarin 6, electrospray ionization (ESI) mass

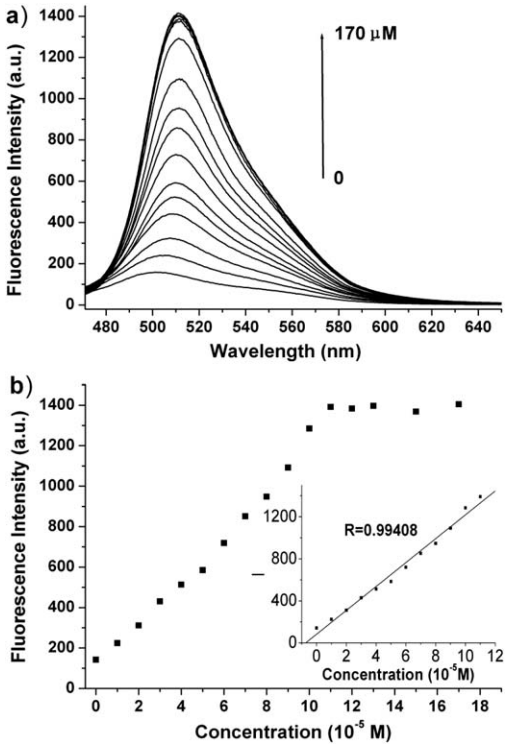

Fig. 5 a) Fluorescence emission spectra ($\lambda_{ex} = 450$ nm) of material **III** (100 ppm) recorded with the addition of *p*-toluenethiol with different concentrations in a citric acid (0.1 M)-phosphate (0.2 M) buffer (pH = 3, ethanol/water = 1/4, v/v). b) Fluorescence intensity at 512 nm against the concentration of *p*-toluenethiol. Inset: a linear portion from 0 μM to 110 μM.

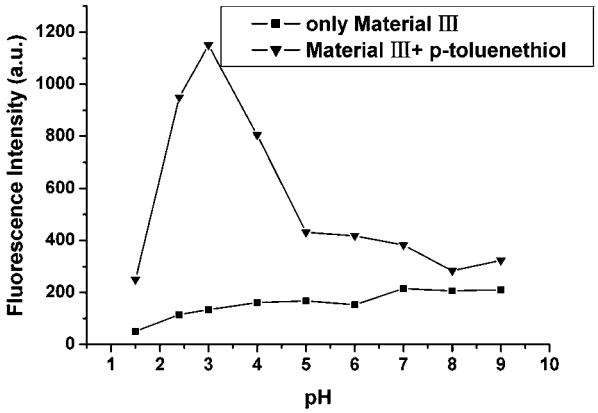

Fig. 6 Fluorescence emission intensity ($\lambda_{em} = 512$ nm) of material III (100 ppm) in the absence and presence of 170 μM *p*-toluenethiol in ethanol/water (1 : 4, v/v) under different pH conditions. The excitation wavelength was at 450 nm. The pH values were maintained by using the following solutions: KCl (0.2 M)-HCl (0.2 M) buffer (pH 1.5), citric acid (0.1M)-phosphate (0.2 M) buffer (pH 2.4–6), HEPES (0.01 M) buffer (pH 7 and 8), Tris-HCl (0.01 M) buffer (pH 9).

spectrometry was carried out to analyze the solution of material **III** titrated with excess *p*-toluenethiol (Fig. S4a†). The peak at *m*/*z* 351.2, corresponding to [coumarin 6 + H]$^+$ (Calc. = 351.1), was clearly observed, indicating that coumarin 6 is released to the solution from material **III**. The reaction product was further isolated and identified to be coumarin 6 by ^{1}H NMR (Fig. S4b†). The conversion mechanism is similar to that reported in our previous work.[62]

The effects of pH values on the sensing performance of our sensing system were investigated. The fluorescence intensity at 512 nm for material **III** with and without *p*-toluenethiol as a function of pH values was shown in Fig. 6. It is found that the emission of material **III** is relatively stable for the pH values ranging from 3 to 9. However, upon the addition of *p*-toluenethiol at a constant concentration of 170 μM, the pH value of the solution affects the emission intensity significantly. The fluorescence enhancement drops a lot as the pH value varies from 3 to 9. This phenomenon could be attributed to the catalysis effect of H^+, which accelerates the oxidization reaction of 2*H*-coumarin 6 to coumarin 6.[62,63] On the other hand, the fluorescence enahncement also decreases at pH < 3 (*e.g.*, pH 1.5), this may be because the 7-diethylamino group of coumarin derivatives is protonized at very acidic pH value, which decreases the fluorescence intensity of coumarin derivatives including coumarin 6.[64,65] Therefore, to improve the signal/noise ratio of the sensing system, a citric acid (0.1 M)-phosphate (0.2 M) buffer at pH 3 was chosen as the detection medium. The finding also implies that material **III** is a particularly attractive chemosensor for some specific environmental monitoring of thiophenols, for instance in highly acidic soils with pH values of 3–4.[66]

To evaluate the selectivity of our sensory system, the fluorescent response of material **III** to a variety of thiols including thiophenols and aliphatic thiols and other common nucleophiles were studied, as illustrated in Fig. 7a. It reveals that only the addition of thiophenols such as *p*-chlorobenzenethiol, *p*-methoxythiophenol, thiophenol and *p*-toluenethiol could result in a prominent enhancement in the fluorescence intensity at 512 nm. In contrast, negligible variations in the emission intensity were observed upon the addition of aliphatic thiols such as cysteine, glutathione and *n*-propylmercapatan. As we know, compared with aliphatic thiols, thiophenols have stronger nucleophilicity and higher affinity to hydrophobic environments. The stronger nucleophilicity could make thiophenols more reactive in the reaction of the disulfide reduction. And the hydrophobicity and π–π stacking interactions provided by the mesopores maybe serve as significant forces to enhance the accessibility of thiophenols over the aliphatic thiols. For other common nucleophiles such as phenol and potassium iodide, there are nearly no fluorescence responses due to the specific reduction of disulfide by thiols. In addition, the emission enhancement by *p*-nitrothiophenol is much smaller than those by other thiophenols. In this case, the thiol nucleophilicity is probably reduced by the electron-withdrawing nitro group, and as a result its reactivity for the S_NAr reaction is weakened. The above observation suggests evidently that our sensory system of material **III** displays a high selectivity for thiophenols.

High selectivity for the analyte in the presence of competing species is a challenging task for practical applications. In this work, we also conducted competition experiments to detect *p*-toluenethiol that was mixed with cysteine, glutathione, *n*-propylmercapatan, glycine, aniline, phenol and potassium iodide, as well as in a mixture of common metal ions such as K^+, Ca^{2+}, Na^+, Zn^{2+}, and Cu^{2+}, respectively. As shown in Fig. 7b, whether or not the competing species exist, obvious emission intensity changes are observed for material **III** upon the addition of *p*-toluenethiol,

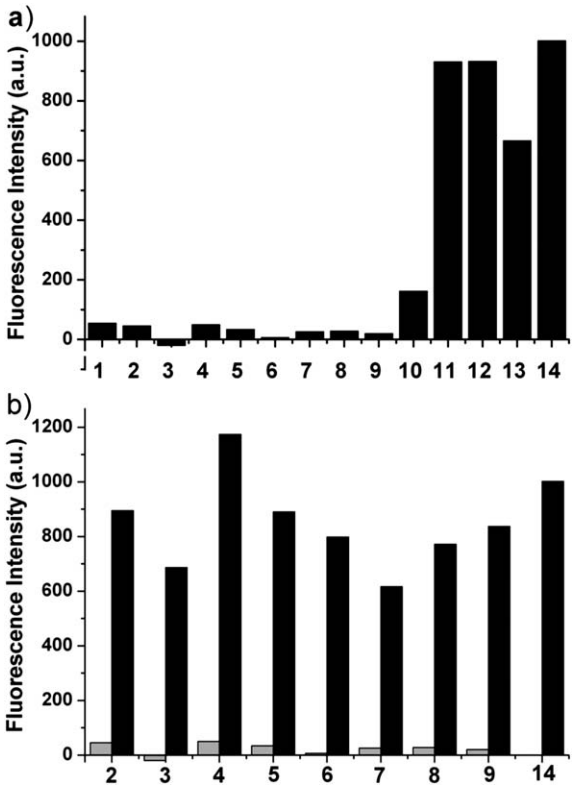

Fig. 7 a) Profiles of fluorescence intensity ($\lambda_{ex} = 450$ nm) variations of material **III** upon the addition of 170 μM of different thiols and nucleophiles. b) The selectivity of material **III** towards thiols and other nucleophiles. Gray bar: the profiles of fluorescence intensity changes at 512 nm in a single analyte at 170 μM with material **III** (100 ppm); Black bar: the profiles of fluorescence intensity changes of a mixture of a nucleophilic reagent at 170 μM and *p*-toluenethiol at 170 μM with material **III** (100 ppm). (1) material **III** only, (2) Cys, (3) GSH, (4) *n*-propylmercapatan, (5) glycine, (6) aniline, (7) phenol, (8) potassium iodide, (9) cations, (10) *p*-nitrothiophenol, (11) *p*-chlorobenzenethiol, (12) *p*-methoxythiophenol, (13) thiophenol, (14) *p*-toluenethiol.

which demonstrates that the detection of thiophenols by material **III** is not affected in the presence of common competing species.

To further illustrate the role of the solid support, controlled experiments using a small molecule **4** as a model compound (Scheme 1b) were performed. Fig. 8 displays the fluorescence response of **4** towards *p*-toluenethiol and cysteine (Cys) with different concentrations or reaction time. Compound **4** shows negligible response for neither *p*-toluenethiol nor Cys under the same measuring condition as that of material **III** (pH 3, 170 μM, 30 min), while similar emission enhancements are observed for *p*-toluenethiol or Cys by prolonging the reaction time to 10 h. On the other hand, the reaction time could be shortened efficiently upon the addition of *p*-toluenethiol with higher concentration (1700 μM). These results indicate that simple molecular **4** exhibits very poor selectivity and sensitivity towards *p*-toluenethiol. Compared with the simple organic molecular **4**, material **III** could provide a large surface area and hydrophobic environment, which could lead to a strong enrichment effect for hydrophobic thiophenols. In addition, the π–π stacking interactions between the coumarin moiety in material **III** and thiophenols could enhance strongly the accessibility of thiophenols

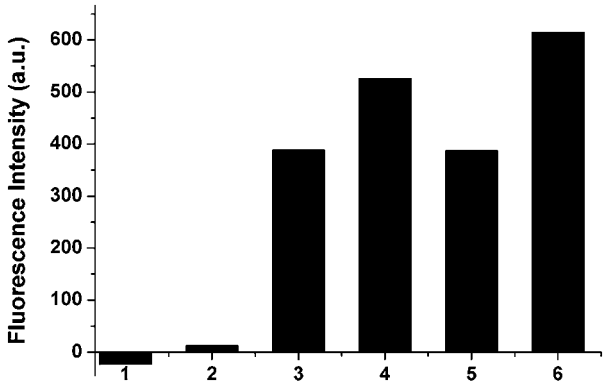

Fig. 8 Profiles of fluorescence intensity ($\lambda_{ex} = 450$ nm) variations at 512 nm of compound **4** (2×10^{-5} M) reacted with *p*-toluenethiol or cysteine (Cys) with different concentrations or reaction time in a citric acid (0.1 M)-phosphate (0.2 M) buffer (pH 3, ethanol/water = 1/4, v/v). (1) 170 μM Cys after 30 min; (2) 170 μM *p*-toluenethiol after 30 min; (3) 170 μM Cys after 10 h; (4) 170 μM *p*-toluenethiol after 10 h; (5) 1700 μM *p*-toluenethiol after 30 min; (6) 1700 μM *p*-toluenethiol after 10 h.

over the aliphatic thiols. All these studies show that the inorganic support indeed presents the synegistic effects and efficiently improves the sensitivity and selectivity of material **III** towards thiophenols.

Conclusions

In summary, we have developed an organic-inorganic hybrid chemosensor material (material **III**) to detect thiophenols based on covalently immobilizing a disulfide-based receptor within the mesopores of MCM-41. Comprehensive characterization techniques demonstrate that the organic fluorophore is grafted inside the mesopores. The material shows high sensitivity and excellent selectivity towards thiophenols over aliphatic thiols and other nucleophiles due to the synergistic effects of the stronger nucleophilicity of thiophenols and the secondary interactions provided by the inorganic support. The detection limit for *p*-toluenethiol is determined to be as low as 7.4×10^{-6} M, which fulfills the requirement for practical applications in the environmental and biological analysis. In the sensing mechanism it was suggested that the disulfide bond is facilely cleaved by thiophenols, and a coumarin-based compound (2*H*-coumarin 6) is released and then spontaneously oxidized to a laser dye (coumarin 6) under ambient conditions. We expect that this work may provide a strategy to design chemical and biological sensors enabling highly selective detection of analytes.

Acknowledgements

This work is financially supported by the National Natural Science Foundation of China (Grant No. 21073213, 20903110), the Main Direction Program of Knowledge Innovation of Chinese Academy of Sciences, the National Basic Research Development Program of China (973 Program) (Grant No. 2007CB936001), and Research Grants Council of Hong Kong SAR (project No. CityU 123607).

References

1 D. T. Quang and J. S. Kim, *Chem. Rev.*, 2010, **110**, 6280.
2 R. Martinez-Manez and F. Sancenon, *Chem. Rev.*, 2003, **103**, 4419.
3 S. K. Kim, D. H. Lee, J. I. Hong and J. Yoon, *Acc. Chem. Res.*, 2009, **42**, 23.
4 L. T. Zeng, P. F. Wang, H. Y. Zhang, X. Q. Zhuang, Q. Dai and W. M. Liu, *Org. Lett.*, 2009, **11**, 4294.
5 S. Mizukami, T. Nagano, Y. Urano, A. Odani and K. Kikuchi, *J. Am. Chem. Soc.*, 2002, **124**, 3920.
6 U. Drechsler, B. Erdogan and V. M. Rotello, *Chem.–Eur. J.*, 2004, **10**, 5570.
7 E. Katz and I. Willner, *Angew. Chem., Int. Ed.*, 2004, **43**, 6042.
8 P. Calero, E. Aznar, J. M. Lloris, M. D. Marcos, R. Martínez-Máñez, J. V. Ros-Lis, J. Soto and F. Sancenón, *Chem. Commun.*, 2008, 1668.
9 S. J. Lee, D. R. Bae, W. S. Han, S. S. Lee and J. H. Jung, *Eur. J. Inorg. Chem.*, 2008, 1559.
10 I. I. Slowing, J. L. Vivero-Escoto, B. G. Trewyn and V. S. Y. Lin, *J. Mater. Chem.*, 2010, **20**, 7924.
11 W. S. Han, H. Y. Lee, S. H. Jung, S. J. Lee and J. H. Jung, *Chem. Soc. Rev.*, 2009, **38**, 1904.
12 S. J. Lee, J. E. Lee, J. Seo, I. Y. Jeong, S. S. Lee and J. H. Jung, *Adv. Funct. Mater.*, 2007, **17**, 3441.
13 Q. Meng, X. Zhang, C. He, G. He, P. Zhou and C. Duan, *Adv. Funct. Mater.*, 2010, **20**, 1903.
14 K. Sarkar, K. Dhara, M. Nandi, P. Roy, A. Bhaumik and P. Banerjee, *Adv. Funct. Mater.*, 2009, **19**, 223.
15 P. Zhou, Q. Meng, G. He, H. Wu, C. Duan and X. Quan, *J. Environ. Monit.*, 2009, **11**, 648.
16 H. J. Kim, S. J. Lee, S. Y. Park, J. H. Jung and J. S. Kim, *Adv. Mater.*, 2008, **20**, 3229.
17 E. Kim, H. Eun Kim, S. Jin Lee, S. Sung Lee, M. Lyong Seo and J. Hwa Jung, *Chem. Commun.*, 2008, 3921.
18 A. B. Descalzo, D. Jimenez, M. D. Marcos, R. Martínez-Máñez, J. Soto, J. El Haskouri, C. Guillém, D. Beltrán, P. Amorós and M. V. Borrachero, *Adv. Mater.*, 2002, **14**, 966.
19 E. Kim, H. J. Kim, D. R. Bae, S. J. Lee, E. J. Cho, M. R. Seo, J. S. Kim and J. H. Jung, *New J. Chem.*, 2008, **32**, 1003.
20 M. Comes, E. Aznar, M. Moragues, M. D. Marcos, R. Martínez-Máñez, F. Sancenón, J. Soto, L. A. Villaescusa, L. Gil and P. Amorós, *Chem.–Eur. J.*, 2009, **15**, 9024.
21 A. B. Descalzo, R. Martínez-Máñez, F. Sancenón, K. Hoffmann and K. Rurack, *Angew. Chem., Int. Ed.*, 2006, **45**, 5924.
22 V. S. Y. Lin, C. Y. Lai, J. G. Huang, S. A. Song and S. Xu, *J. Am. Chem. Soc.*, 2001, **123**, 11510.
23 A. B. Descalzo, K. Rurack, H. Weisshoff, R. Martinez-Manez, M. D. Marcos, P. Amoros, K. Hoffmann and J. Soto, *J. Am. Chem. Soc.*, 2005, **127**, 184.
24 M. Comes, M. D. Marcos, R. Martínez-Máñez, F. Sancenón, J. Soto, L. A. Villaescusa, P. Amorós and D. Beltrán, *Adv. Mater.*, 2004, **16**, 1783.
25 S. Basurto, T. Torroba, M. Comes, R. Martínez-Máñez, F. Sancenón, L. Villaescusa and P. Amorós, *Org. Lett.*, 2005, **7**, 5469.
26 A. B. Descalzo, M. D. Marcos, R. Martínez-Máñez, J. Soto, D. Beltrán and P. Amorós, *J. Mater. Chem.*, 2005, **15**, 2721.
27 K. Shimada and K. Mitamura, *J. Chromatogr., Biomed. Appl.*, 1994, **659**, 227.
28 J. C. Love, L. A. Estroff, J. K. Kriebel, R. G. Nuzzo and G. M. Whitesides, *Chem. Rev.*, 2005, **105**, 1103.
29 R. Dubinskii, I. Krivtsova, N. Grigor'ev, E. Degterev, L. Filimonova and M. Kalinkina, *Pharm. Chem. J.*, 1994, **28**, 942.
30 F. E. C. George and D. Clayton, *Patty's Industrial Hygiene and Toxicology*, New York, 4th edn, 1994, 2, 4336.
31 R. P. Verma, S. Kapur, O. Barberena, A. Shusterman, C. H. Hansch and C. D. Selassie, *Chem. Res. Toxicol.*, 2003, **16**, 276.
32 Health Council of the Netherlands: Committee on Updating of Occupational Exposure Limits. *Benzenethiol; Health-based Reassessment of Administrative Occupational Exposure Limits*. The Hague: Health Council of the Netherlands, 2004; 2000/15OSH/095.
33 R. Munday, *J. Appl. Toxicol.*, 1985, **5**, 402.
34 T. P. Heil and R. C. Lindsay, *J. Environ. Sci. Health, Part B*, 1989, **24**, 349.
35 Interim acute exposure guideline levels (AEGLs) for phenyl mercaptan (C_6H_5SH), Interim 1: 11/2007 US Environmental Protection Agency.
36 EPA Method 8270C, Semivolatile Organic Compounds by Gas Chromatography/mass spectrometry (GC/MS) US Environmental Protection Agency, December, 1996.
37 X. Chen, Y. Zhou, X. J. Peng and J. Yoon, *Chem. Soc. Rev.*, 2010, **39**, 2120.
38 J. Bouffard, Y. Kim, T. M. Swager, R. Weissleder and S. A. Hilderbrand, *Org. Lett.*, 2008, **10**, 37.
39 P. Pullela, T. Chiku, M. Carvaniii and D. Sem, *Anal. Biochem.*, 2006, **352**, 265.
40 Y.-B. Ruan, A.-F. Li, J.-S. Zhao, J.-S. Shen and Y.-B. Jiang, *Chem. Commun.*, 2010, **46**, 4938.
41 J. V. Ros-Lis, B. Garcia, D. Jimenez, R. Martinez-Manez, F. Sancenon, J. Soto, F. Gonzalvo and M. C. Valldecabres, *J. Am. Chem. Soc.*, 2004, **126**, 4064.
42 W. Lin, L. Yuan, Z. Cao, Y. Feng and L. Long, *Chem.–Eur. J.*, 2009, **15**, 5096.
43 H. S. Hewage and E. V. Anslyn, *J. Am. Chem. Soc.*, 2009, **131**, 13099.
44 L. Yi, H. Li, L. Sun, L. Liu, C. Zhang and Z. Xi, *Angew. Chem., Int. Ed.*, 2009, **48**, 4034.
45 W. Lin, L. Long and W. Tan, *Chem. Commun.*, 2010, **46**, 1503.
46 W. Jiang, Q. Fu, H. Fan, J. Ho and W. Wang, *Angew. Chem., Int. Ed.*, 2007, **46**, 8445.
47 W. Jiang, Y. Cao, Y. Liu and W. Wang, *Chem. Commun.*, 2010, **46**, 1944.
48 A. M. Piggott and P. Karuso, *Anal. Chem.*, 2007, **79**, 8769.
49 B. Zhu, X. Zhang, Y. Li, P. Wang, H. Zhang and X. Zhuang, *Chem. Commun.*, 2010, **46**, 5710.
50 J. H. Lee, C. S. Lim, Y. S. Tian, J. H. Han and B. R. Cho, *J. Am. Chem. Soc.*, 2010, **132**, 1216.
51 S. Huh, J. W. Wiench, B. G. Trewyn, S. Song, M. Pruski and V. S. Y. Lin, *Chem. Commun.*, 2003, 2364.
52 M. H. Lim and A. Stein, *Chem. Mater.*, 1999, **11**, 3285.
53 B. G. Trewyn, I. I. Slowing, S. Giri, H. T. Chen and V. S. Y. Lin, *Acc. Chem. Res.*, 2007, **40**, 846.
54 D. R. Radu, C.-Y. Lai, J. Huang, X. Shu and V. S. Y. Lin, *Chem. Commun.*, 2005, 1264.
55 V. Dufaud and M. E. Davis, *J. Am. Chem. Soc.*, 2003, **125**, 9403.
56 J.-S. Wu, W.-M. Liu, X.-Q. Zhuang, F. Wang, P.-F. Wang, S.-L. Tao, X.-H. Zhang, S.-K. Wu and S.-T. Lee, *Org. Lett.*, 2007, **9**, 33.
57 J. Q. Wang, L. Huang, M. Xue, Y. Wang, L. Gao, J. H. Zhu and Z. G. Zou, *J. Phys. Chem. C*, 2008, **112**, 5014.
58 M. Llusar, G. Monrós, C. c. Roux, J. L. Pozzo and C. m. Sanchez, *J. Mater. Chem.*, 2003, **13**, 2505.
59 X. W. Wu, J. F. Ruan, T. Ohsuna, O. Terasaki and S. N. Che, *Chem. Mater.*, 2007, **19**, 1577.
60 B. Wang, C. Chi, W. Shan, Y. Zhang, N. Ren, W. Yang and Y. Tang, *Angew. Chem., Int. Ed.*, 2006, **45**, 2088.
61 H. Jin, Z. Liu, T. Ohsuna, O. Terasaki, Y. Inoue, K. Sakamoto, T. Nakanishi, K. Ariga and S. Che, *Adv. Mater.*, 2006, **18**, 593.
62 R. Sheng, J. Ma, P. Wang, W. Liu, J. Wu, H. Li, X. Zhuang, H. Zhang and S. Wu, *Biosens. Bioelectron.*, 2010, **26**, 949.
63 K. H. Grellmann and E. Tauer, *J. Am. Chem. Soc.*, 1973, **95**, 3104.
64 A. V. Pinheiro, A. J. Parola, P. V. Baptista and J. C. Lima, *J. Phys. Chem. A*, 2010, **114**, 12795–12803.
65 S. Aoki, M. Shiro and E. Kimura, *Chem.–Eur. J.*, 2002, **8**, 929–939.
66 T. Gunnlaugsson, T. Clive Lee and R. Parkesh, *Tetrahedron*, 2004, **60**, 11239.

